

SOURCE SPECTRA, MOMENT, AND ENERGY FOR RECENT EASTERN MEDITERRANEAN EARTHQUAKES: CALIBRATION OF INTERNATIONAL MONITORING SYSTEM STATIONS

Kevin M. Mayeda, Abraham Hofstetter,* Arthur J. Rodgers, and William R. Walter
Lawrence Livermore National Laboratory and *Geophysical Institute of Israel

Sponsored by U.S. Department of Energy
Office of Nonproliferation and National Security
Office of Defense Nuclear Nonproliferation
National Nuclear Security Administration

Contract No. W-7405-ENG-48

ABSTRACT

In the past several years there have been several large ($M_w > 7.0$) earthquakes in the eastern Mediterranean region (Gulf of Aqaba, Racha, Adana, etc.), many of which have had aftershock deployments by local seismological organizations. In addition to providing ground truth data ($GT \ll 5$ km) that is used in regional location calibration and validation, the waveform data can be used to aid in calibrating regional magnitudes, seismic discriminants, and velocity structure. For small regional events ($m_b \ll 4.5$), a stable, accurate magnitude is essential in the development of realistic detection threshold curves, proper magnitude and distance amplitude correction processing, formation of an M_s - m_b discriminant, and accurate yield determination of clandestine nuclear explosions.

Our approach provides a stable source spectra from which M_w and m_b can be obtained without regional magnitude biases. Once calibration corrections are obtained for earthquakes, the coda-derived source spectra exhibit strong depth-dependent spectral peaking when the same corrections are applied to explosions at the Nevada Test Site (Mayeda and Walter, 1996), chemical explosions in the recent "Depth of Burial" experiment in Kazakhstan (Myers et al., 1999), and the recent nuclear test in India. For events in the western U.S. we found that total seismic energy, E , scales as $M_o^{0.25}$ resulting in more radiated energy than would be expected under the assumptions of constant stress-drop scaling. Preliminary results for events in the Middle East region also show this behavior, which appears to be the result of intermediate spectra fall-off ($f^{-1.5}$) for frequencies ranging between ~ 0.1 and 0.8 Hz for the larger events. We developed a Seismic Analysis Code (SAC) coda processing command that reads in an ASCII flat file that contains calibration information specific for a station and surrounding region, then outputs a coda-derived source spectra, moment estimate, and energy estimate.

This is Lawrence Livermore National Laboratory document number UCRL-JC-138990.

Key Words: regional coda waves, moment, energy, SAC

OBJECTIVE

For sparse local and regional seismic networks a stable magnitude is of utmost importance for establishing accurate seismicity catalogs and assessing seismic hazard potential. In the context of network capability, we need accurate magnitudes for construction of detection threshold curves, a crucial element of nuclear test monitoring. In this paper we describe a method of calibrating a region for coda envelope processing using a new routine in SAC. Unlike magnitudes such as M_L , M_d and m_b which are relative, narrowband measures that often have regional biases, our approach can provide a stable absolute source spectra that is corrected for S-to-coda transfer function, scattering, and anelastic attenuation and site effect. Because coda envelope amplitude measurements are not as sensitive to 3-D path heterogeneity and source radiation pattern, the resultant spectra can then be used for stable moment estimation (and hence M_w), traditional short-period magnitudes (i.e., m_b , M_L) and radiated seismic energy, E . There have been numerous scattering studies over the past 3 decades investigating the mechanisms that control coda generation and its decay with time from the origin and dependence upon distance. For our method however, we only use an empirical approach to fit the observed envelopes to obtain an amplitude measure over a range of narrow

frequency bands. We then empirically tie these amplitudes to independently derived moment estimates from calibration events through a simple boot-straping procedure. Past studies for earthquakes in the western United States showed that a single coda envelope amplitude measurement was roughly equivalent to a 64 station network using direct waves (Mayeda & Walter, 1996). For explosions at the Nevada Test Site (NTS) we found that a 1 Hz single-station coda measurement was roughly equivalent to a 20 station network using direct L_g or P_n (Mayeda, 1993). This is the result of making a time domain measurement over a large length of coda, thereby averaging the combined effects of source radiation pattern, path heterogeneity, and near site random interference, all of which can affect individual phases such as L_g and P_n . The results of the frequency-dependent calibration have been used as input into a newly developed interactive SAC command that forms narrowband envelopes, measures amplitudes, applies region and station-specific corrections, outputs ASCII source information (e.g., M_w , m_b , $\Delta\sigma$, E) and plots the moment-rate spectra. In this paper we describe the calibration method, then apply it to a data set in the Middle East region to estimate seismic moment (and M_w), total radiated seismic energy, and dynamic stress drop (e.g., Orowan) (see Figure 1). We then compare with previous results from the western United States (Kanamori et al., 1993, Mayeda and Walter, 1996).

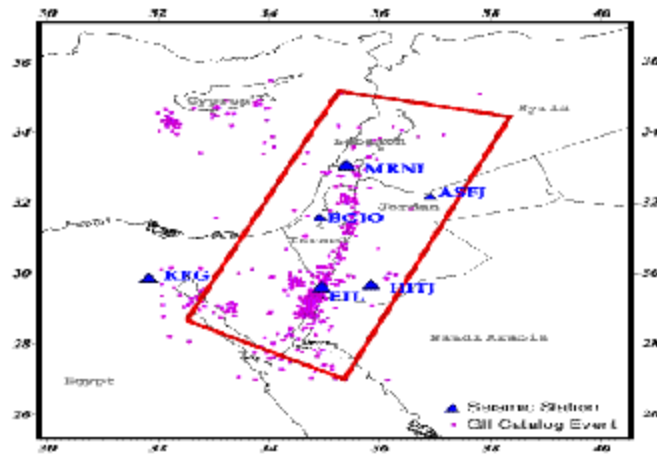


Figure 1 Map showing regions, broadband stations and seismicity from the Gil catalog.

RESEARCH ACCOMPLISHED

Synthetic Envelopes

We found that a simple analytic form that resembles the single-scattering model of Aki (1969) generally does a good job at fitting both regional and local coda envelopes. The main difference is that we found that we had better fits by forming the envelopes relative to the S arrival, not the origin time as is done in most scattering models. The analytic expression that we used to fit the observed narrowband envelopes at center frequency f is

$$A_c(f, t | x) = A_o \cdot H(t - \frac{x}{v(x)}) \cdot (t - \frac{x}{v(x)})^{-g} \cdot \exp(-b \cdot (t - \frac{x}{v(x)})) \quad (1)$$

where A_o is a source constant, H is the Heaviside step function, t is the time in seconds from the origin, x is the distance in kilometers, $v(x)$ is the velocity of the peak arrival in km/sec and g and b control the coda decay. It should be noted however that the more complex 2-D and 3-D multiple scattering models could also be used (see Sato and Fehler review, 1999). For our purposes we only want an empirical fit to the data

over a range of distances and frequency bands and thus this simple form is completely adequate for this purpose.

Since we are not explicitly applying a scattering model that has attenuation built into its formulation, we need to find an empirical distance relation for the coda amplitudes. This is preferable since we do not want to make any assumptions about homogeneous coda decay in a region, an assumption commonly made in past coda studies. Instead, we fold in both geometrical spreading and attenuation (whether it be from scattering, absorption, leakage etc.) using a strictly empirical form. We reiterate that we use equation 1 as a means of matching the observed coda envelope shape to extract a coda amplitude measurement. In essence, equation 1 is used as an empirical metric and thus any functional relationship could have been used that fits the data. The steps described in this paper allow one to measure coda envelopes, which are initially in dimensionless units, correct for distance and site effects and tie to an absolute measure. The validation of this approach is simple. We verify that we obtain the same source spectra at different stations and distances for the same event (thus confirming our empirical distance corrections) and then verify that our inferred moments are the same as those that were independently determined from other means such as long-period waveform modeling.

Coda Envelopes

For our data we applied an 8th order, zero-phase (four poles, two passes) Butterworth filter for 13 narrow frequency bands ranging between 0.03 and 8.0 Hz for the two horizontal components. This range of frequency bands was chosen such that we could compute M_w for the Gulf of Aqaba mainshock of November 22, 1995 (M_w 7.1) and measure the high frequencies of some of the smaller aftershocks.

For each component the narrowband envelope at center frequency f is of the form:

$$e(t | f) = \sqrt{(v(t)^2 + h(t)^2)} \quad (2)$$

where $v(t)$ is one of the bandpass filtered seismograms and $h(t)$ is its corresponding Hilbert transform. We then take the \log_{10} of the envelopes, average the two horizontal envelopes, then smooth. Fig. (2) shows an example of a broadband trace and a selection of envelopes in different narrow frequency bands. It is preferable to use the horizontal elements since S-waves have better signal-to-noise ratio and averaging the two provides a smoother envelope than a single component alone. Of course this processing could also be done on a single component such as the vertical but is less desirable.

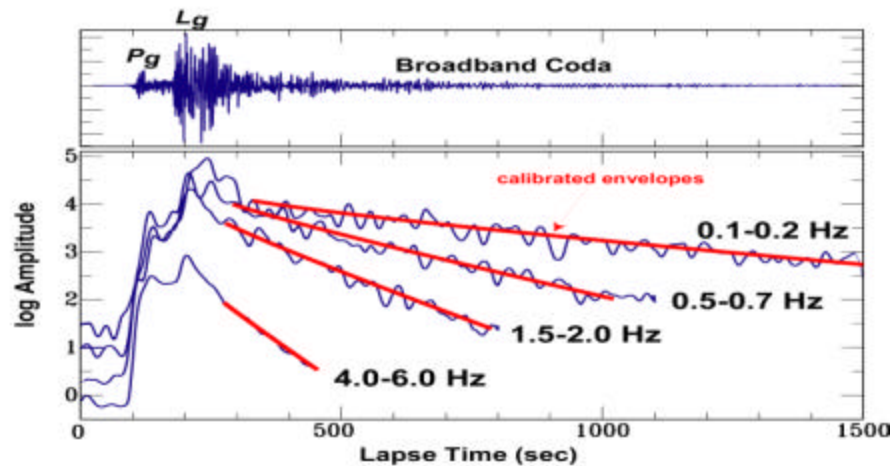


Figure 2. Example of broadband waveform and selected narrowband envelopes along with calibrated envelopes.

Velocity of Direct Phase

After forming narrowband envelopes for all the events, we measure the (phase) velocity of the peak S-arrival for each frequency band and plot versus distance. For the longest periods the peak corresponds to the Rayleigh or Love waves but because we empirically correct for each frequency band, mixing wavetypes makes no difference on the final results as will be shown in the concluding sections. Since our goal is to calibrate both local and regional distance earthquakes, we find that a simple second-order polynomial fits the data at all distances. For each frequency the distant-dependent velocity, v is of the form,

$$v(x | f) = \text{velorder}_0 + \text{velorder}_1 \cdot x + \text{velorder}_2 \cdot x^2 \quad (3)$$

where velorder_0 , velorder_1 and velorder_2 are constants.

Coda Shape Factors

Now that we know the velocities for each frequency band, we can fit our simple analytic form to find the coda shape parameter b which controls the coda decay as measured from the direct S (or L_g) arrival. By rearranging equation 1 and taking the \log_{10} of both sides we get,

$$\log_{10} \left[A_c(f, t | x) \cdot \left(t - \frac{x}{v(x)} \right)^g \right] = \log_{10} \left(A_o \cdot H \left(t - \frac{x}{v(x)} \right) \right) - b \cdot \left(t - \frac{x}{v(x)} \right) \cdot \log(e) \quad (4)$$

We let g vary from 0 to 2 and found that fixing $g=0.7$ fit the data well for the entire frequency range. Coincidentally, this value is consistent with other scattering formulations that consider surface wave and

body wave scattering in a full-space. By plotting equation 4 versus $\left(t - \frac{x}{v(x)} \right)$, the slope of the best

fitting line is $b \log(e)$.

Since we want to fit the coda at all distances we try to measure the coda over a range of distances to determine if b is dependent upon distance. For the higher frequencies b is strongly distant dependent whereas for frequencies below ~ 0.5 Hz, the coda shape factor is roughly constant and is smaller (i.e., decays more slowly than the higher frequencies). We find that a simple linear form fits the b values as a function of distance x spanning both local and regional distances,

$$b(x | f) = b_o(f) + \eta x \quad (5)$$

where $b_o(f)$ is the intercept value at zero distance at center frequency f and η is the slope.

Simple Distance Corrections

For events in the Dead Sea rift and Gulf of Aqaba region, the Geophysical Institute of Israel (GII) routinely performs network locations and assorted magnitudes such as m_b , M_L and M_w . Now that we have the velocities and coda shape factors we set A_o in equation (1) to unity, take the \log_{10} to be consistent with our observed envelopes, then dc shift the synthetic envelopes to fit the observed envelopes using an L-1 norm. The magnitude of the dc shift is the non-dimensional coda amplitude. This amplitude is analogous to a direct wave measure in the sense that a distance and site correction still need to be made. Measuring the coda envelope amplitude over a length of time merely provides a more stable measure than using direct waves which are of short duration and thus considerably more susceptible to interference, source-station heterogeneity, and source radiation pattern. In the following paragraph we empirically find the distance dependence for each frequency band, apply it to the data, then validate by comparing measurements of the same event at two different stations.

For each frequency band we subtract the M_L from the amplitude and plot versus distance in kilometers. We try to use events in a narrow magnitude range for each frequency band when determining the distance corrections to avoid potential biases related to corner frequency scaling. For example, using only small

events at short distances and only large events at longer distances would result in very biased curve fitting as opposed to using events of roughly the same size. Up to this point we can now measure distance-corrected coda amplitudes from narrowband envelopes but these are still in dimensionless units. Figure (3a) shows a cartoon of non-dimensional coda spectra for hypothetical earthquakes of various sizes and its corresponding figure shows what the spectra will look like after correcting to an absolute scale. The goal is to correct for S-to-coda transfer function and site effects to obtain a moment-rate spectra. Again, these amplitudes are relative to a source amplitude of 1.0 and are thus in dimensionless units and must be corrected to an absolute scale. The following section describes this crucial series of steps.

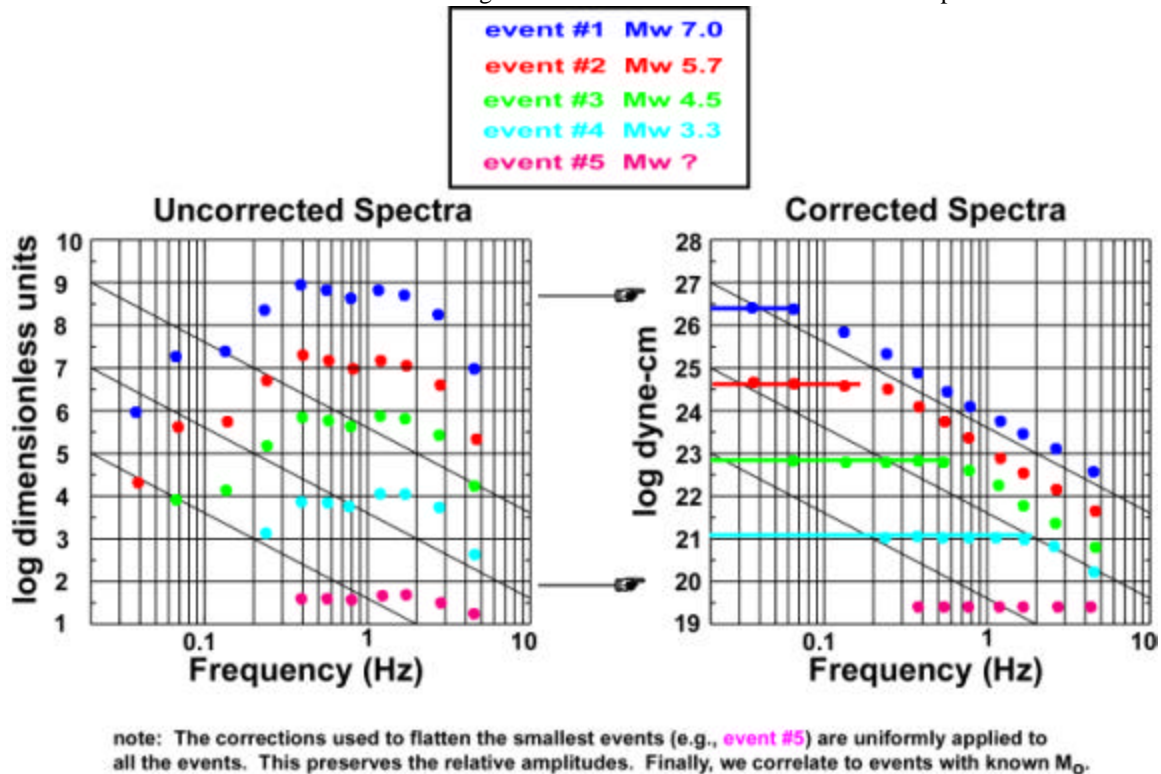


Figure 3a and 3b. Non-dimensional coda amplitude corrected for distance effect only (fig. 3a) for a range of events. Figure 3b shows corrected spectra after tying to independent moments and applying Green's function corrections.

Green's Function and Seismic Moment Corrections

Up to this point we have measured non-dimensional coda envelope amplitudes and corrected for distance. In this section we relate these values to an absolute scale, namely seismic moment to obtain a moment-rate spectrum. Our only assumption is that the S-wave source spectrum is flat below the corner frequency. We purposely underestimate where the corner frequency lies for our set of calibration events to avoid flattening our spectra unrealistically.

We used a 1-D reflectivity code to waveform model a series of events in the region to estimate seismic moment. The only assumption we make is that the source spectrum of these events is flat below the corner frequency. As shown in Figure (3b), we add constants to all amplitudes for each frequency band such that the seismic moments, in a least squares sense, agree with the waveform modeled results. Since these are frequency-dependent corrections, independent of distance, the corrections must be uniformly applied to all distance-corrected amplitudes. Figure (3b) shows that with conservative estimates of the corner frequency, we can flatten the spectra for a range of event sizes. For events that are too small to be waveform modeled ($< \sim M_w 3.5$), we can still estimate moment using periods less than a few Hertz. For especially small events ($\sim M_w 2.5$) we can assume they have flat source spectrum at least to 10 Hz. This use of the very small

events is essentially a Green's function correction that allows us to extend the stable coda-derived source spectrum to much smaller events. Therefore, this allows us to find the amplitude corrections for the frequencies between ~2.0 and 8 Hz. Though in figures (3a & 3b) we use just a few events for illustrative purposes, for the actual data we used a number of events of the same relative size to come up with the best set of moment corrections. In our case we instrument deconvolved the traces beforehand and converted to velocity. However, if the instrument did not change over the range of time of study, the moment corrections (which include site and S-to-coda transfer function) could have also included the instrument response.

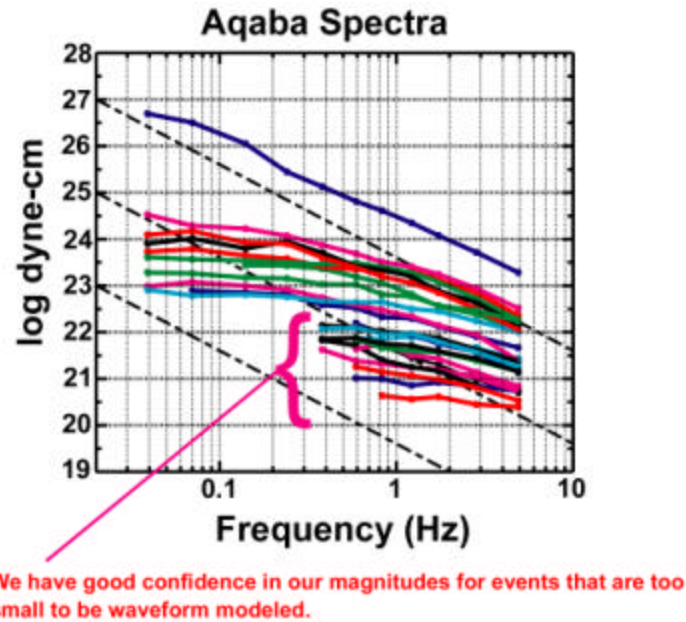


Figure 4. Selected moment-rate spectra for the Gulf of Aqaba sequence.

TESTING & VALIDATION

Figure (4) shows selected source spectra for events in the Gulf of Aqaba region along with some events from the Dead Sea rift at station BGIO. We test for consistency by comparing spectra of the same event at two different stations, in our case, stations BGIO in Israel and KEG in Egypt. Figure (5) shows spectra for two events, one is nodal at BGIO and the other is not. In both cases, the spectra at KEG and BGIO are virtually identical, despite a significant source radiation pattern difference. If we compare individual amplitudes for a large number of events, we also see that the inter-station variation is also very small, comparable to what was observed at NTS.

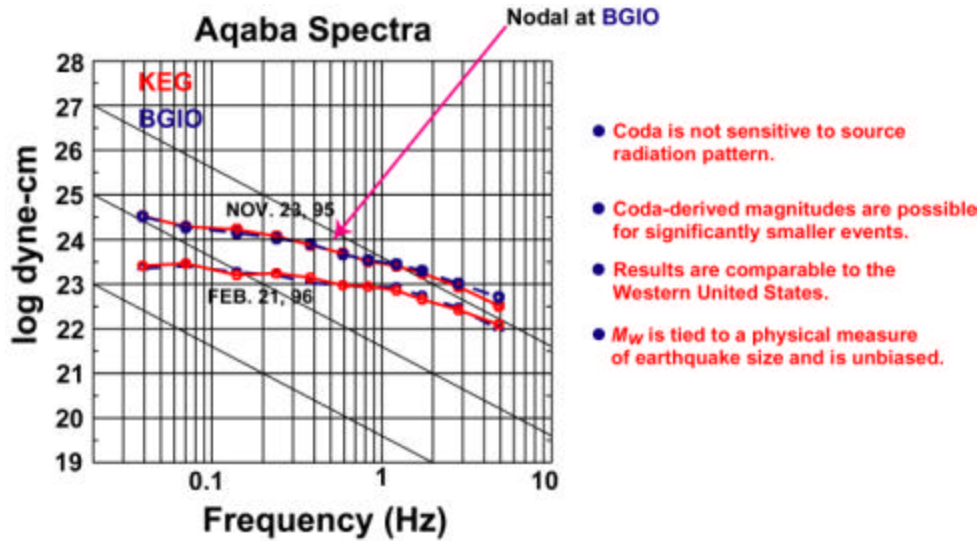


Figure 5. Spectra recorded at KEG and BGIO for the same two events show little variation. Note: The November 23, 1995 aftershock is nodal at BGIO but the coda-derived spectra is the same as the spectra at KEG.

Finally, we verify that our absolute amplitudes are correct by computing M_w from the lowest frequencies of our measured spectra and comparing against independent M_w 's. Figure (6) shows that there is good agreement between the two approaches.

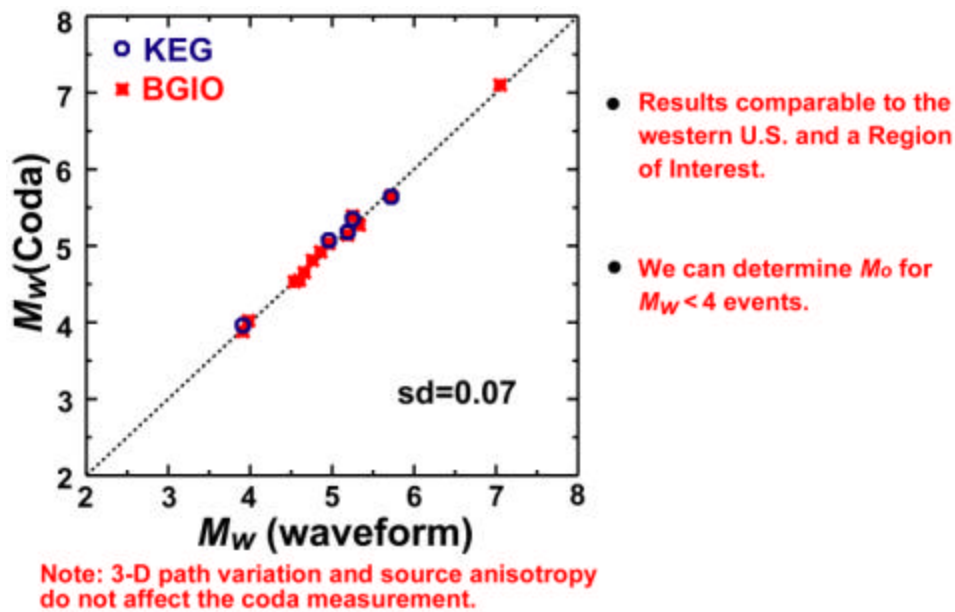


Figure 6. As was found in the western United States, the coda-derived M_w agrees with waveform modelling results.

CONCLUSIONS & RECOMMENDATIONS

Now that we have verified that our spectra are completely corrected back to the S-wave source, we can begin to address a long-standing problem in observational seismology, namely accurate estimation of the radiated seismic energy. For events for which we observe a flat, long-period level (proportional to moment) and decaying high frequencies, we need to extrapolate our observed spectra to $f=0$ and $f=\infty$. Though a majority of the energy is near the corner frequency, for completeness we must do this extrapolation. For the long periods we extend our spectra to $f=0$ Hz and for the high frequencies, we assume an omega square decay to $f=\infty$. Next, we convert our spectra to velocity by dividing by omega, then square and integrate. Only those events for which we have measured at least 70% of the total S-wave energy are used. Finally, we assume a P-wave contribution of energy by multiplying by 1.07. From Figure 7 we see that the Gulf of Aqaba events follow the same trend as those from the western United States.

We have successfully transported a methodology for calibrating stations for regional magnitude to International Monitoring System (IMS) stations in the Middle East region. Resultant source spectra show very small interstation variation as was found in the western U.S. and will allow accurate estimates of M_w and m_b for small regional events that cannot be measured teleseismically. We are systematically calibrating all the IMS stations in the region and are tying regional m_b 's to the teleseismic m_b . The coda-derived M_w estimates are being used as input to the joint LANL/LLNL MDAC code for discrimination calibration. The coda methodology has been incorporated into the newest version of SAC that will allow amplitude measurements on narrowband coda envelopes given a calibration flatfile.

Radiated Seismic Energy and Orowan Stress Drop

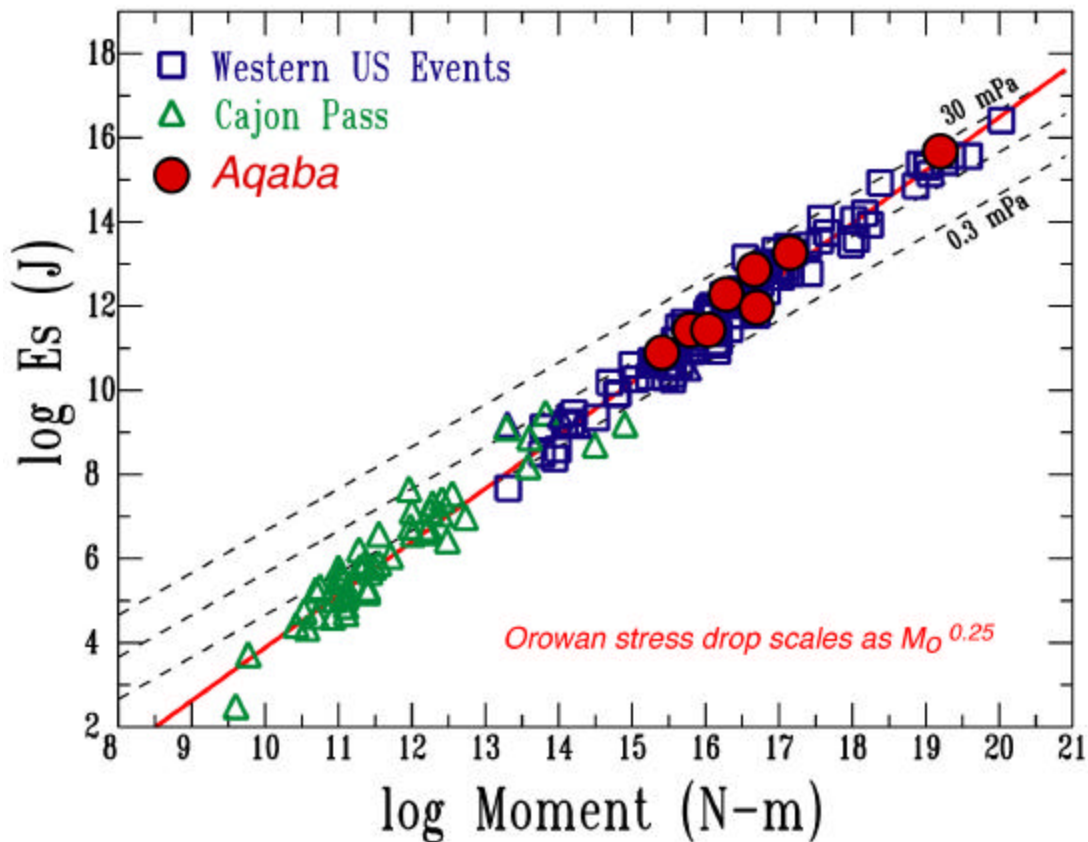


Figure 7. Energy-moment relationship for Aqaba events is in good agreement with results from the western United States.

REFERENCES

Aki, K. (1969), Analysis of the seismic coda of local earthquakes as scattered waves, *J. Geophys. Res.*, **74**, 615-631.

Kanamori, J., J. Mori, E. Hauksson, T. H. Heaton, L. K. Hutton, and L. J. Jones (1993), Determination of of earthquake energy release and ML using TERRAScope, *BSSA*, **83**, 330-346.

Mayeda, K., 1993, mb(LgCoda): A stable single station estimator of magnitude, *BSSA*, **83**, 851-861.

Mayeda, K. and W. R. Walter, 1996, Moment, energy, stress drop and source spectra of western United States earthquakes from regional coda envelopes, **101**, *J. Geophys. Res.* 11195-11208.

Myers, S. C., W. R. Walter, K. Mayeda, and L. Glenn (1999), Observations in support of Rg scattering as a source for explosion S waves: Regional and local recordings of the 1997 Kazakhstan Depth of Burial experiment, *BSSA*, **89**, 544-549.